Characteristics and numerical simulation of maize ear threshing under mixed airflow

Xinping Li†*, Yanan Li†, Bin Peng, Shendi Xu, Junyi Wang, Ruizhe Sun, Jiarui Hou
(*College of Agricultural Equipment Engineering, Henan University of Science and Technology, Luoyang 471003, Henan, China*)

Abstract: To make up for the gap in the research on high water content maize threshing by airflow, this study took high-speed, low flow, low-speed high flow airflow, and high water content maize ear as the research basis. The variation of air flow impacted threshing in numerical simulation, and the variation process of smoke visualization in the threshing area was compared. Taking the maize ear direction, the angle between the maize ear and the air pipe, the diameter of the air pipe, and the flow rate of the air compressor as factors, single-factor and quadratic regression orthogonal rotation combination tests were carried out, and the parameters were optimized. Finally, high-speed photography was used to shoot the maize kernels' shelling process, and movement rules were analyzed from both the front and side views. The results showed that the velocity changes of each section under the numerical simulation are consistent with the flow state changes of smoke. The velocity reached its maximum on the circumference of the maize ear surface and presented a symmetrical distribution. Due to the velocity gradient and pressure gradient difference, the high-speed airflow would entrain the phenomena of the low-speed airflow. When the transverse maize ear, the angle between the maize and the airflow tube) was 45°, the diameter of the airflow tube was 7 mm, the flow rate of the airflow tube was 33 m/s, the loose amount was 10 pieces, the threshed amount was 15 pieces, and the damage rate was below 3%. Through high-speed photography, it was found that the cyclic force circle was destroyed after the maize kernel fell off, the motion of the removed maize kernel was similar to the oblique throwing motion, and the threshing process was carried out in the unit of "arrangement unit". The threshing process followed the "arrangement law", and the threshing track was "spiral". The results of this research can provide ideas for the mechanical design and development of high-moisture-content maize threshing by air.

Keywords: maize ear, impact threshing, numerical simulation, airflow, high moisture content
DOI: 10.25165/j.ijabe.20251803.9220

Citation: Li X P, Li Y N, Peng B, Xu S D, Wang J Y, Sun R Z, et al. Characteristics and numerical simulation of maize ear threshing under mixed airflow. Int J Agric & Biol Eng, 2025; 18(3): 265–275.

1 Introduction

As an important economic and food crop, maize plays an essential role in agricultural production and development and is significant in people's daily lives and economic development[1-4]. However, the high damage rate and loss rate of grain have become one of the factors restricting the development of the agricultural industry[5,6]. Currently, the primary processing of maize ears mainly relies on mechanical harvesting and machining. However, some problems exist, such as low efficiency, high energy consumption, and high grain loss rate[7-11].

At present, many researchers have studied the threshing and processing of high-water-content maize, but most of them rely on mechanical methods[11-15]. The threshing method of high moisture content maize by airflow is still in the blank stage, but airflow has been developed in the agricultural field. Ghafori et al.[16] investigated the physical and conveying properties of maize and barley using an aspirated pneumatic conveying system. It was found that the mechanical damage of the two kinds of seeds increased linearly with the increase in air velocity. Nguyen et al.[17] dried the potato by airflow. The air-drying dynamics of the sample were mathematically described using different mass transfer models (internal, external, and mixed). It was found that external mass transfer dominated at low air speeds, while the mixed model better represented the experimental data for higher speeds. Chai et al.[18] addressed the issue of uneven lateral distribution of threshed material on the cleaning screen of tangential axial flow threshing drums by developing an adaptive guide rod system. Shang et al.[19] tested the noise of combine harvesters using a spiral acoustic array and identified the primary noise sources by employing noise source identification technology based on sound pressure distribution. The test results showed that the noise of the collector was mainly concentrated in the frequency range of 1-4 kHz. Airflow is involved in the agricultural field of grain cleaning, drying, harvesting, processing, etc. However, there is little research on the threshing of maize with high moisture content, and the research on airflow in the threshing of maize with high moisture content is at a blank stage[5,20-23].

Li et al.[3,24,25] studied the arrangement of maize kernels and the principle of staggered joints and lapping. They found the "arrangement unit" and "ABA gap identical principle" and called

Received date: 2024-07-13 **Accepted date:** 2025-04-09
Biographies: Yanan Li, PhD candidate, research interest: new institution, new theory of agricultural machinery, Email: LI1516359758@126.com; **Bin Peng**, MS candidate, research interest: agricultural machinery and intelligent equipment, Email: 220320261824@stu.haust.edu.cn; **Shendi Xu**, MS candidate, research interest: agricultural machinery and intelligent equipment, Email: 201430030120@stu.haust.edu.cn; **Junyi Wang**, MS candidate, research interest: agricultural machinery and intelligent equipment, Email: 15139042158@163.com; **Ruizhe Sun**, MS candidate, research interest: agricultural machinery and intelligent equipment, Email: 18639156721@163.com; **Jiarui Hou**, MS candidate, research interest: agricultural machinery and intelligent equipment, Email: rjdj888813@163.com.
†The authors contributed equally to this work.
***Corresponding author: Xinping Li**, Professor, research interest: agricultural products processing and harvesting machinery. College of Agricultural Equipment Engineering, Henan University of Science and Technology. Tel: +86-13592065522, Email: aaalxp@163.com.

the arrangement law of maize kernels the "arrangement law". Based on the two kinds of airflow and the cooperative carrying capacity of the maize arrangement unit, the circulating force circle, and the maize, this paper made a comparative analysis by comparing the velocity changes of the flow field in the maize threshing area and the state of the airflow under visual smoke, carried out the quadratic orthogonal rotation combination test with single factor and multiple factors, and optimized the working parameters. The transmission and consumption process of maize's transverse force chain network under the impact of airflow were analyzed by high-speed photography on the threshing movement process and law, which fills the gap in the application of airflow in high-moisture-content maize threshing.

2 Stress analysis of maize kernel

The lift and drag effects of mixed air on maize kernels were analyzed by vertically impacting the surface of maize ear with mixed airflow, and the force was simplified as horizontal velocity $v_x = v\cos\tau$ and vertical velocity $v_y = v\sin\tau$. The airflow force between maize kernels was analyzed, as shown in Figure 1.

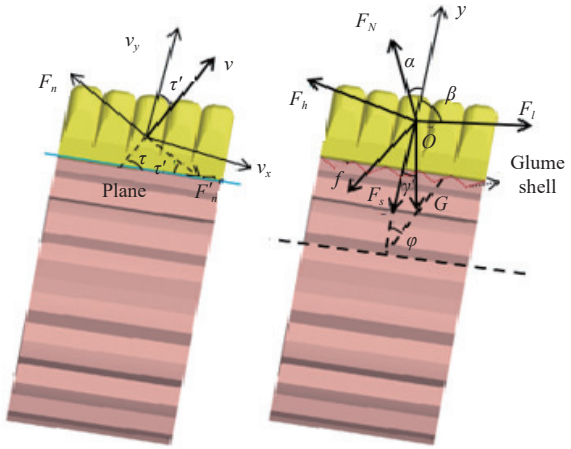

Note: α is the angle between the supporting force and the y-axis; β is the angle between airflow, extrusion pressure, and y-axis; γ is the angle between gravity and the y-axis; F_n is the supporting force of glume shell on grain when the angle is α; f is the friction force of the glume shell on the grain when the angle is α; F_h and F_l are the extrusion pressure of the dislocation lap; F_β is the maximum flow rate of airflow in the impact area; G is maize kernel gravity; F_1 is the connection force between the kernel and the maize cob; S is the transverse contact plane area; v is the impact area velocity; τ is the angle between the maize kernels and the plane where the tangent line is located.

Figure 1 Stress analysis of maize kernel

When maize is moving obliquely upward, the total average resistance of the airflow on the upper surface of the maize is

$$F_N = \frac{3}{2}\rho s v_x^2 \sin^2\tau = \frac{3}{2}\rho s v^2 \cos\tau^2 \sin^2\tau \quad (1)$$

where, F_N is the resistance of the airflow to the maize kernels, N; ρ is the airflow density, kg/m^3; s is the contact area between the maize kernels and the airflow, m^2; v is the airflow velocity, m/s; τ is the angle between the direction of kernel movement and the tangential horizontal plane, (°).

The transverse component of the normal force F'_n is

$$F = -F'_N \sin\tau = -\frac{3}{2}\rho s v^2 \sin^3\tau\cos^2\tau \quad (2)$$

where, F is the lateral component of the normal force, N.

Combined with the total average resistance of Equation (1) and the force of airflow on the lower surface, when the airflow impact force is transmitted transversely, in addition to the airflow impact force, the maize kernels are also subject to the glume shell supporting force, the surrounding maize kernel extrusion pressure, the carpopodium connection force, the gravity of the maize kernels themselves, and the friction between the glume shell and the kernel. Then the total force under the transverse airflow maize shilling is as follows:

$$F_m = n\left[(F_h - F_l)\sin(\beta) + \int_{\alpha_1}^{\alpha_2} F_n \sin(\alpha)\,d\alpha + \int_{\alpha_1}^{\alpha_2} f\,|\sin(\alpha)|\,da + + G\sin(\gamma) + F_\beta \sin(\beta) - \frac{3}{2}\rho s v^2 \sin^3\tau\cos^2\tau\right] \quad (3)$$

where, F_m is the force acting on threshing, N; n is the amount of maize kernels; α is the angle between the supporting force and the y-axis, (°); β is the angle between the squeezing force and the y-axis, (°); γ is the angle between gravity and the y-axis, (°); F_n is the supporting force of the glumes on the kernels when the angle is α, N; f is the frictional force of the glumes on the kernels when the angle is α, N; F_h and F_l are the squeezing forces of the maize kernels on both sides, N; G is gravity, N; F_s is the connection force between the maize kernels and the maize cobs, N.

When a single maize kernel is stressed, it shifts and squeezes the surrounding maize kernels, and the forces transfer to each other, causing the maize kernel to thresh gradually.

3 Materials and methods

3.1 Test materials and equipment

The maize variety used in the experiment was Boyun 88. After drying, the maize was controlled according to the same water classification, and the water content was measured according to GB/T3543.6. The mean water content was in the range of 25.8%-27.5%.

The leading test equipment is the JNY-20A air compressor, which is used for gas compression and providing airflow power; the XGB-2200 high-pressure vortex fan, which provides auxiliary power for air threshing; the AS836 digital anemometer for measuring airflow velocity; American Phantom Miro series LC111 high-speed digital camera, resolution 1 280 800, maximum shooting rate 400 000 frames/s, sensitivity ISO-12232 SAT, minimum exposure time 2 μs. The electronic angle ruler is used to measure the angle between the maize and the flow tube (the angle between the transverse tangent line and the flow tube axis and the angle between the longitudinal axis and the flow tube axis). Combined with the above test equipment, a multi-angle airflow discrete maize ear test rig was built, as shown in Figure 2.

3.2 Test methods

The soft Workbench module of Fluent was used to analyze the impact flow field of maize ears under the airflow tube, and the velocity of different sections under the airflow impact was analyzed. Through the visual smoke test under airflow coupling, different colors of smoke were injected into the air compressor airflow pipe and vortex fan pipe (diameter 70 mm) to make the two airflows show different colors. The smoke was separately injected into the vortex fan duct before and after startup to analyze the influence of air compressor airflow on the surrounding airflow; the smoke of two different colors was separately injected into the air compressor airflow duct and the vortex fan pipe to analyze the state of the two airflows coupled with each other. The impact area was determined according to the smoke trace. The above three methods were used to compare and analyze the airflow's shape and impact

process and the flow field's numerical simulation through high-speed photography. In the above three methods, the angle between the air compressor air pipe and the vortex fan was set at 15°, the wind speed of the vortex fan was kept constant at 10 m/s, the length of the air compressor air pipe was 10 cm, and the two airflow directions were perpendicular to the maize axis. Finally, the effect of airflow on threshing was analyzed by comparing the velocity variation of the flow field and the process of smoke movement.

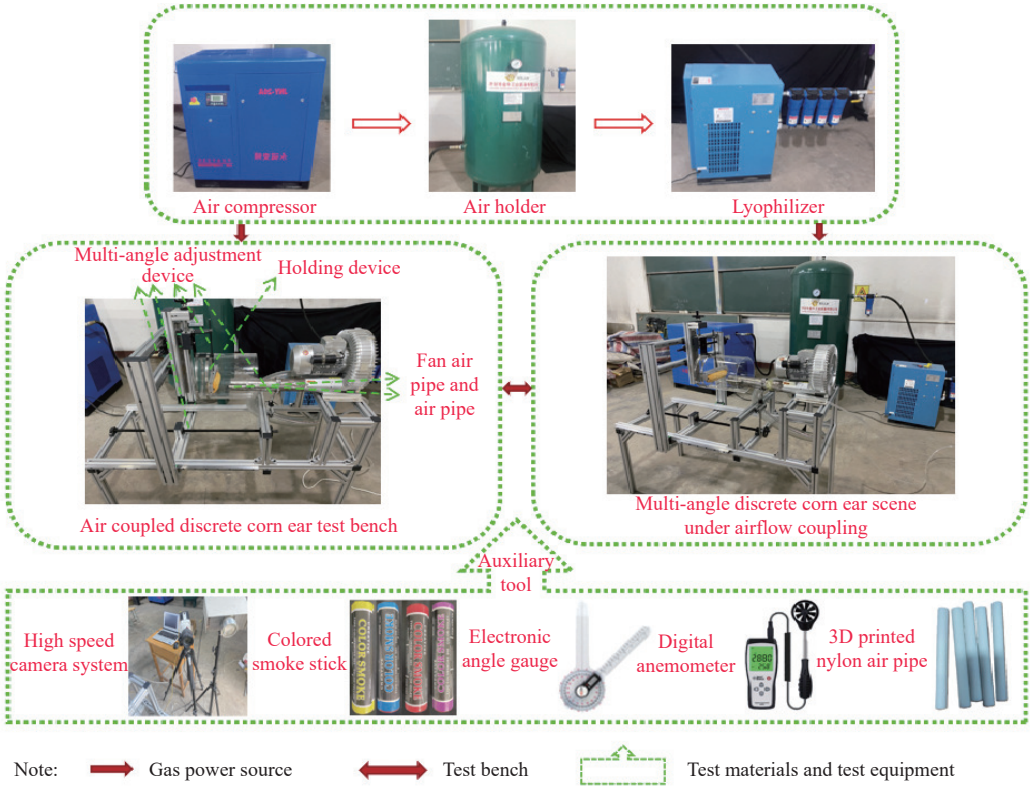

Figure 2 Airflow multi-angle discrete maize ear test bench

In the single-factor and multi-factor tests, the angle x_1 between the maize and airflow coupling tube, the diameter x_2 of the air compressor airflow tube, and the wind speed x_3 were taken as the test factors, respectively. At the right end of the test bench, a coupling flow tube between the vortex fan and the air compressor is arranged, and the vortex fan is used as an auxiliary flow. The rotation angle of the air pipe clamping device and the clamping device is adjustable. A high-speed camera was placed on the side of the test unit. After the experiment stopped, the seeds were dispersed, the seeds that fell were collected, and the data were recorded. Five tests were carried out at each factor level, and the average value of the test index was taken. The test index took the maize kernels loosening amount e and threshing amount y_1 as the test index and the crushing rate y_2 as the observation index (excluding the test index). The maize kernel crushing rate was shown in Equation (4) through the control variable method test. Maize kernels loose amount y_1 (referring to the number of maize kernels loose) and threshed amount y_2 (referring to the number of maize kernels threshed) were taken as test indices, and the crushing rate y_3 was taken as the observation index (not included in the test index). The test was carried out using the control variable method. The crushing rate of maize kernels was as Equation (4):

$$Z_s = \frac{m_s}{m_i} \times 100\% \tag{4}$$

where, Z_s is the crushing rate, %; m_s is the crushing mass, g; m_i is the total mass of the sample, g.

4 Test process and analysis

4.1 Numerical simulation analysis of airflow field

Airflow is a fluid flow whose mass, momentum, and energy follow the conservation law, reflecting the conservation of physical quantities per unit of time and volume. It is used to represent the universal variable. It can be expressed as:

$$\frac{\partial(\rho\Delta)}{\partial t}+\frac{\partial(\rho u\Delta)}{\partial x}+\frac{\partial(\rho v\Delta)}{\partial y}+\frac{\partial(\rho w\Delta)}{\partial z}= \frac{\partial}{\partial x}\left(\Lambda\frac{\partial\Delta}{\partial x}\right)+\frac{\partial}{\partial y}\left(\Lambda\frac{\partial\Delta}{\partial y}\right)+\frac{\partial}{\partial z}\left(\Lambda\frac{\partial\Delta}{\partial z}\right)+s \tag{5}$$

where, Λ is the generalized diffusion coefficient; Δ is the general variable; u, v, and w are the components of vector u in the x, y, and z directions; s is the generalized source term.

The software Fluent used the finite volume method to solve the discretization of the governing equations. The end face of the vortex fan pipe and the air compressor pipe inlet was the working fluid inlet, the boundary of the air inlet was the velocity inlet, and the other side was the outlet. The model was simplified to analyze the flow field change when the air blows to the maize, as shown in Figure 3.

Considering the structure of the model in this study, an automatic mesh division was adopted, with a total of 4 373 358 nodes and 24 526 250 units. Non-slip surface boundary conditions and standard surface roughness models were adopted. Based on the Reynolds number of airflow velocity, the turbulence intensity was determined to be 0.05 and the turbulence viscosity coefficient to be 10, and the improved QUICK scheme was adopted. The RNG turbulent model was selected, and turbulent Flow dominates the model. Therefore, the Swirl Dominate Flow option was selected, and the SIMPLE solution algorithm was used to achieve better convergence and facilitate calculation. Specific simulation parameters are listed in Table 1.

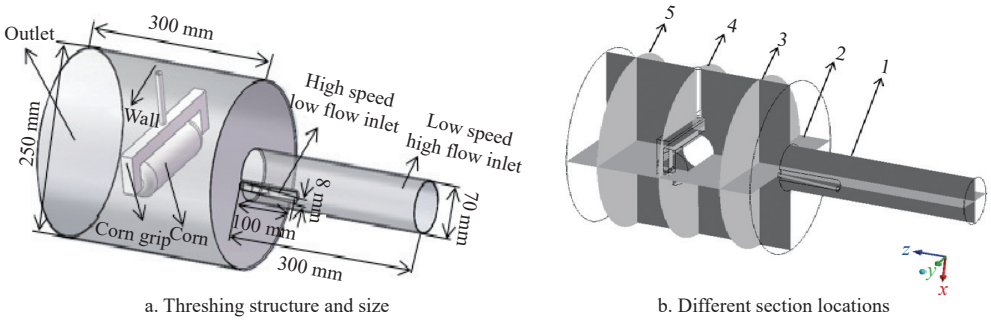

a. Threshing structure and size b. Different section locations

Figure 3 Threshing mechanism and different section positions

Table 1 Numerical simulation parameters

Parameter	Quantitative value
Inlet wind speed 1/m·s^{-1}	10
Inlet wind speed 2/m·s^{-1}	30
Inlet current intensity/%	5
Inlet hydraulic diameter 1/mm	70
Inlet hydraulic diameter 2/mm	8
Outlet torrent intensity/%	4
Outlet hydraulic diameter/mm	250
Surface roughness thickness/mm	0
Surface roughness	0.5
Accuracy of convergence of operational equations	10^{-4}
Relaxation factor momentum	0.7
Relaxation factor turbulent kinetic energy	0.8
Relaxation factor turbulent kinetic energy dissipation	0.3

Different sections of the device were extracted with the maize centroid as the origin to analyze the flow field distribution in the threshing area, as shown in Figure 3b. Sections 1 and 2 were the flow field regions in the *XZ* and *YZ* planes, respectively. Section 3 was the *XY* plane closest to the airflow inlet. Section 4 was the *XY* plane, where the centroid of maize was located. Section 5 was the *XY* plane closest to the maize outlet, and the spacing distance of Sections 3, 4, and 5 was 100 mm.

According to Figure 4, the analysis of Section 1 in the *XZ* plane showed that the maximum velocity cloud map of the maize surface in Regions *a* and *b* was symmetrically distributed along the *Z*-axis, and the maximum velocity values were all on the maize surface along the *X*-axis. The reason was that the airflow was obstructed by an approximate cylinder shape and was diffused on the circumference surface, its direction was deflected, and the velocity accelerated on the surface, increasing. The maximum speed value was the area where the threshing effect was noticeable. When connected with Regions *a* and *b*, the maize surface in Region *c* forms a specific low-speed vortex around the maize in the *X*-axis direction because the maize surface blocks the airflow. When the airflow hits the surface, the direction is deflected. The speed would be reduced, and the low-speed and high-flow air would have a noticeable wrapping effect on the maize surface. In Region *d*, the airflow was blocked by maize, and the direction and velocity of the airflow were deflected and

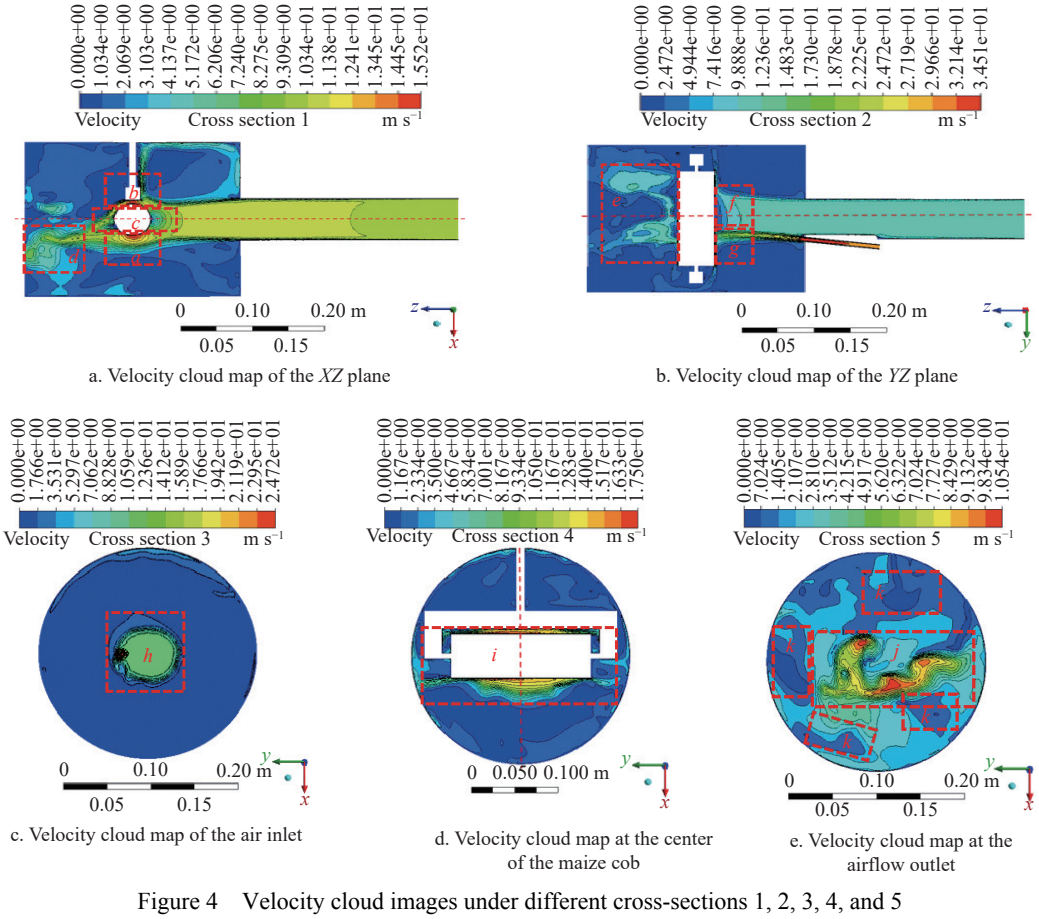

a. Velocity cloud map of the *XZ* plane b. Velocity cloud map of the *YZ* plane

c. Velocity cloud map of the air inlet d. Velocity cloud map at the center of the maize cob e. Velocity cloud map at the airflow outlet

Figure 4 Velocity cloud images under different cross-sections 1, 2, 3, 4, and 5

fluctuated. The velocity presented a gradient distribution in the *Z*-axis direction, forming a turbulent region.

According to the analysis of Section 2 in the *YZ* plane, it could be seen that Region *e* and Region *f* were approximately symmetrically distributed along the *Z*-axis, and the maize surface blocked the airflow to form a low-speed vortex. The reason was that when the surface blocked the airflow, the flow velocity weakened, the surrounding pressure changed, and the flow velocity presented a gradient distribution. However, the velocity was significantly lower than that of Region *g*, indicating that the force mainly acts on the maize surface, which is suitable for air threshing. For Region *g*, which was close to the velocity inlet and had a fast velocity, when the airflow impacted the surface of the maize, the velocity slowed down, but the impact area became more extensive. Combined with the velocity of Region *f* in the direction of the *Z*-axis, it could be seen that due to the velocity difference between some low-speed, high-flow airflow and high-speed, low-flow airflow, the high-speed airflow could be surrounded by low-speed airflow, reducing air dissipation and having an essential impact on maize threshing.

Sections 3, 4, and 5 were distributed from near to far from the airflow inlet, where Section 3 Region *h* was the area of high velocity and low flow and ground velocity and high flow. From the direction of the *Z*-axis perpendicular to the section, there was a noticeable speed and step difference between low-speed and low-flow airflow, resulting in low-speed airflow wrapping around high-speed airflow. To a certain extent, the dissipation of the high-speed airflow was reduced. For Region *i* of Section 4, the velocity cloud map was symmetrically distributed along the *X*-axis, where the surface velocity value was the largest, and the velocity on both sides of the maize obstructed by the surface gradually decreased. However, there was a specific velocity gradient, and its fluctuation can achieve threshing better. For Region *j* of Section 5, the section at this time was closer to the exit of the flow field. After the airflow passed over the surface of the maize, it gradually approached the outlet, and at this time, the pressure gradually approached the atmospheric pressure. Its direction and velocity were deflected and fluctuated, and the velocity was distributed in a gradient, thus forming a turbulent flow. Region *k* was affected by the central turbulent flow region and the surface of the flow field, forming a difference between velocity and pressure and gradually forming a low-speed vortex in the area near the surface of the flow field. The turbulent flow field in this section could better transport maize kernels.

4.2 Visual smoke test under airflow coupling

The mixing pattern of airflow and impact area has an important impact on the performance of air threshing. High-speed photography was used to analyze the mixing pattern of airflow. The interval of each selected image was 0.0115 s, and three images were selected to analyze the smoke traces left by airflow mixing and impact on maize and analyze the impact area of airflow and the coverage area of auxiliary airflow.

It could be seen from Figure 5a that the smoke in the vortex fan pipe impacted by high-speed airflow was initially loose and irregular. As the smoke continued to be applied in the vicinity and direction of the airflow tube, according to Bernoulli's principle, due to the velocity and pressure difference between the airflow tube and the surrounding air, the surrounding smoke gradually accumulated near the high-speed airflow. When the airflow becomes stable, the smoke gradually jets to the surface of the maize in a cone shape, resulting in the smoke gradually accumulating towards the center of the airflow driven by the high-speed airflow. In the virtual frame, the area with the light color of the smoke jet trace was the gathering area when the airflow impacted this area at high speed, and the surrounding color was darker, indicating that the surrounding airflow was greatly affected by the high-speed airflow.

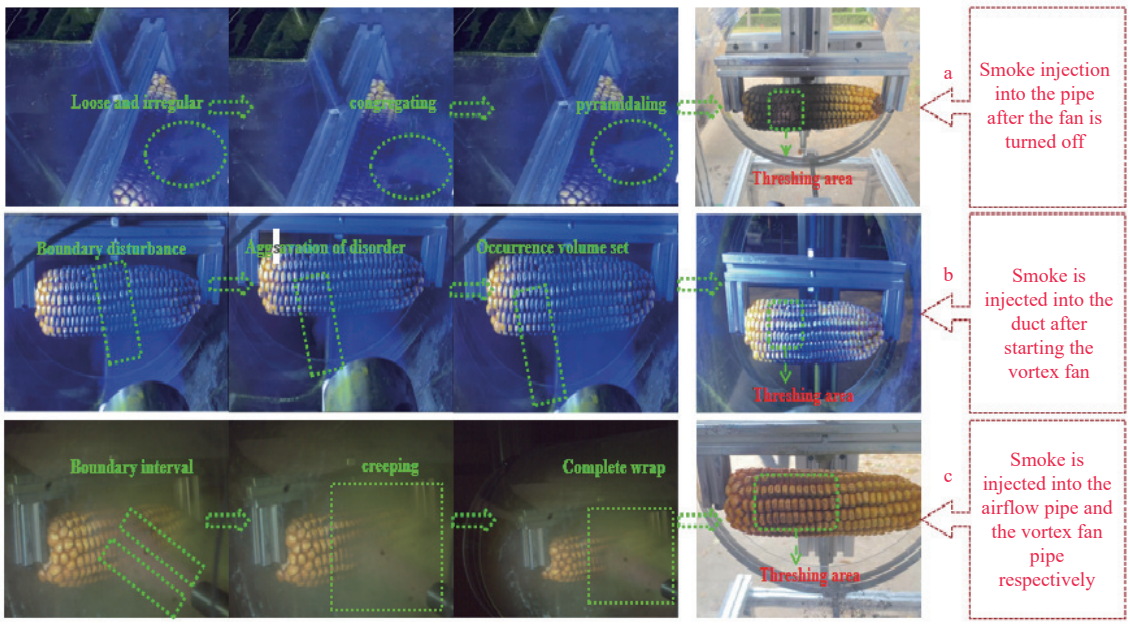

a. 10.036 s b. 10.049 s c. 10.061 s Threshing area

Figure 5 Three kinds of smoke experiments in the visual state

As shown in Figure 5b, after the smoke was blown out by the vortex fan, under the action of high-speed airflow, the boundary smoke was affected by the high-speed airflow and gradually presented a turbulent state. In the coupling process of high-speed airflow and low-speed airflow, the two would collide, and the high-speed and low-flow airflow would gradually roll up the low-speed and high-flow air, and the smoke boundary would be destroyed under the high-speed airflow. With the continuous impact of the

airflow, the boundary disturbance phenomenon becomes more and more apparent. The high-speed airflow seriously enrolled the boundary smoke, and the low-speed airflow gradually enshrouded the high-speed air. When impacting the maize region, the lighter color area was the threshing area, and the surrounding darker color area was the auxiliary air impact area, indicating that when the high-speed air surrounded by the low-speed air impacted the maize ear, the low-speed air played an auxiliary role in the maize threshing.

As shown in Figure 5c, under the coupling of high-speed, low, and low-speed high flow, there was an apparent boundary between pink smoke and yellow smoke. There was a velocity difference and pressure difference in the initial coupling stage. The low-speed air stream gathered with the high-speed air stream, and its wrapping effect was gradually enhanced until it was completely wrapped around the high-speed air stream. High-velocity airflow had a strong breakdown effect because of its high speed and small cross-sectional area. Under continuous impact, the binding effect of high-speed air on low-speed air was enhanced, which reduced the dissipation of high-speed air and enhanced the impact force. It was found that the color between the gaps was darker, and the kernel's surface color was lighter, indicating that the impact of high-speed airflow played the main role in threshing. In contrast, low-speed airflow played an auxiliary role, and the effect of high-speed airflow on low-speed airflow was noticeable.

4.3 Single- and multi-factor test and optimization analysis

Through the single-factor test, the factor range was as follows: the angle between the maize and air compressor air pipe was 10°-80°, the diameter of the air compressor air pipe was 5-10 mm, and the flow rate of the air compressor air pipe was 25-35 m/s. Through analysis, it was found that the angle between the maize and the airflow tube, the diameter of the airflow tube, and the airflow velocity significantly affected the threshing amount and loose amount of maize. Moreover, the loose amount and the loose amount of maize were better than the longitudinal threshing amount, and the threshing effect was better, which provided a preliminary screening for the factor level of the orthogonal test[10].

An orthogonal experimental design was conducted using the center composite design of the response surface method in Design-Expert 13.0 software[26,27]. The experimental factors and levels are listed in Table 2.

Table 2 Multi-factor horizontal coding

Level	Angle between maize and air compressor flow pipe x_1/(°)	Pipe diameter x_2/mm	Air compressor flow rate x_3/m·s^{-1}
−1.682	15	6	27
−1	30	7	29
0	45	8	31
1	60	9	33
1.682	75	10	35

The air-coupled discrete maize ear test bench was used for the threshing test, and each index under different parameter combinations was counted. The test scheme and results are listed in Table 3, and the index data weres averaged by three repetitions.

The Design-Expert software was used to fit test factors and indicators and analyze variance; the significance of test indicators of factors was tested. Regression equations of loose and threshed amounts were obtained based on regression analysis, and the influence of interaction terms on test indicators was analyzed using the response surface. The results of the variance analysis are listed in Table 4.

Table 3 Design scheme and results of the quadratic orthogonal rotation combination test

Class number	Angle between maize and flow pipe x_1/(°)	Pipe diameter x_2/mm	Pipe velocity x_3/m·s^{-1}	Test index		Observation index
				Loose amount y_1/pieces	Threshing amount y_2/pieces	Breakage rate y_3/%
1	−1	−1	−1	10	5	0
2	1	−1	−1	6	6	0
3	−1	1	−1	7	7	0
4	1	1	−1	9	8	0.1
5	−1	−1	1	9	12	0
6	1	−1	1	9	14	0.1
7	−1	1	1	8	7	0
8	1	1	1	13	9	0
9	−1.682	0	0	7	5	0.2
10	1.682	0	0	8	7	0
11	0	−1.682	0	13	10	0.1
12	0	1.682	0	15	7	0
13	0	0	−1.682	5	9	0
14	0	0	1.682	7	16	0.2
15	0	0	0	9	11	0
16	0	0	0	9	10	0
17	0	0	0	9	11	0
18	0	0	0	10	12	0.1
19	0	0	0	10	12	0
20	0	0	0	10	10	0
21	0	0	0	10	11	0
22	0	0	0	10	10	0
23	0	0	0	10	11	0.1

As can be seen from Table 4, the experimental model of loose quantity was highly significant (p<0.0001). The Angle of the air flow pipe x_1, the diameter of the air flow tube x_2, and the airflow velocity x_3 on the loose amount of maize ears were very significant (p<0.01). The interaction term x_1x_2 of the angle between the maize and airflow tube and the diameter of the airflow tube, and the interaction term x_1x_3 of the angle between the maize and the airflow tube and the flow rate of the airflow tube had very significant effects on the loose amount of maize ears (p<0.01).

The interaction term x_2x_3 of air tube diameter and flow velocity significantly affected the loose amount of maize (p<0.05). In addition, the quadratic term x_1^2 of the angle between the maize and the airflow tube, the quadratic term x_2^2 of the diameter of the airflow tube, and the quadratic term x_3^2 of the flow rate of the airflow tube also had significant effects on the loose amount of maize ear (p<0.01). According to the size of the F-value, each factor's main order of influence on the loose quantity is x_3, x_2, x_1.

For the same reason, it can be seen from Table 4 that the experimental model of threshing quantity is highly significant (p<0.0001). The effects of angle x_1, diameter x_2, and flow velocity x_3 on the loose amount of maize ears were very significant (p<0.01). The interaction term x_2x_3 of airflow tube diameter and flow velocity had significant effects on the threshing amount of maize ears (p<0.01). The quadratic term x_1^2 of the angle between the maize and the flow tube and the quadratic term x_2^2 of the flow tube diameter had significant effects on the loose amount of maize ears (p<0.01). The quadratic term t of the flow rate of the air pipe had x_3^2 significant effect on the ear-loose amount of maize (p<0.05), while the other items were not significant. According to the F-value, the main order of the influence of each factor on the loose amount was as follows: x_3, x_2, and x_1.

Table 4 Variance of ear loose amount and threshed amounts of maize

Source	Loose volume					Threshing amount				
	Sum of squares	df	Mean square	*F*-value	*p*-value	Sum of squares	df	Mean square	*F*-value	*p*-value
Model	109.65	9	12.18	56.90	<0.0001	166.12	9	18.46	43.37	<0.0001
x_1	1.60	1	1.60	7.50	0.0169	6.42	1	6.42	15.09	0.0019
x_2	2.97	1	2.97	13.285	0.0026	8.93	1	8.93	20.99	0.0005
x_3	7.86	1	7.86	36.73	<0.0001	56.48	1	56.48	132.72	<0.0001
x_1x_2	15.13	1	15.13	70.64	<0.0001	0.0000	1	0.0000	0.0000	1.0000
x_1x_3	6.13	1	6.13	28.60	0.0001	0.5000	1	0.5000	1.17	0.2981
x_2x_3	1.13	1	1.13	5.25	0.0392	24.50	1	24.50	57.57	<0.0001
x_1^2	10.69	1	10.69	49.92	<0.0001	51.93	1	51.96	122.11	<0.0001
x_2^2	34.70	1	34.70	162.08	<0.0001	13.58	1	13.58	31.91	<0.0001
x_3^2	28.98	1	28.98	135.35	<0.0001	3.81	1	3.81	8.95	0.0104
Residual	2.78	13	0.2141			5.53	13	0.4256		
Lack of fit	0.7836	5	0.1567	0.6269	0.6851	0.6433	5	0.1287	0.2105	0.9486
Pure error	2.00	8	0.2500			4.89	8	0.6111		
Cor total	112.43	22				171.65	22			

Note: df is the degree of freedom.

The missing fitting terms of the model in Table 4 were insignificant (p>0.1), indicating that the regression model was valid. After the non-significant factors are removed, the regression equations of each factor on the loose amount and the threshed amount are shown in Equations (6) and (7):

$$y_1 = 9.67 + 0.3428x_1 + 0.466x_2 + 0.7589x_3 + 1.38x_1x_2 + 0.875x_1x_3 + 0.375x_2x_3 - 0.8202x_1^2 + 1.48x_2^2 - 1.35x_3^2 \ (R^2 = 0.9752) \quad (6)$$

$$y_2 = 10.9 + 0.6856x_1 + 0.8088x_2 + 2.03x_3 - 1.75x_2x_3 - 1.81x_1^2 - 0.9245x_2^2 + 0.4897x_3^2 \ (R^2 = 0.9678) \quad (7)$$

The response analysis diagram of the interaction item to the test index is shown in Figure 6. For the loose amount y of maize kernels, the interaction terms of the diameter of the air duct and the angle between maize and the air duct affected the loose amount, as shown in Figure 6a. When the flow rate of the air duct was 31 m/s, and the angle between the maize and the air duct was constant, the loose amount decreased first and then rose with the increase of the diameter of the air duct. This was because the cross-sectional area and flow rate of the air duct increase with the increase of the diameter of the pipe. The impact force was not enough to destroy the force chain in the region, and the loosening effect was poor. The volume flow rate and the air coverage area increase with the diameter of the airflow pipe, the stability of the force chain and the

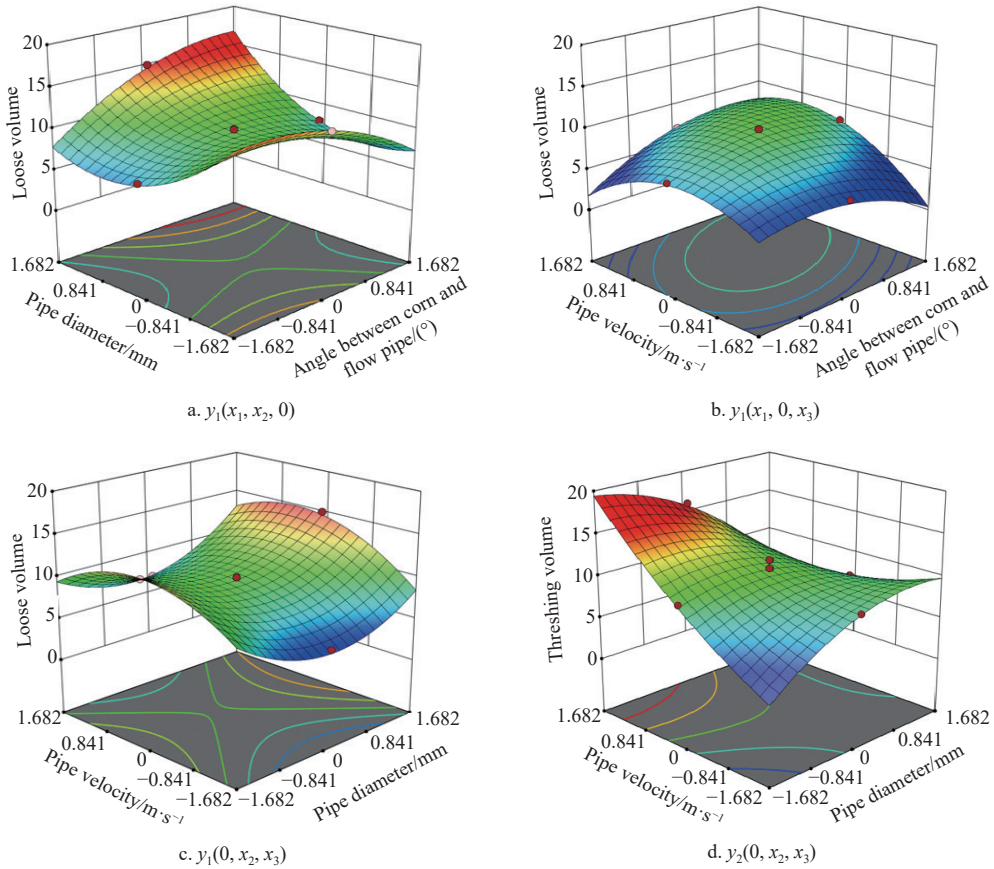

a. $y_1(x_1, x_2, 0)$ b. $y_1(x_1, 0, x_3)$

c. $y_1(0, x_2, x_3)$ d. $y_2(0, x_2, x_3)$

Figure 6 Influence of interaction term on loose amount and threshing amount

affected area becomes more extensive, and the degree of looseness increases. When the diameter of the airflow tube was constant, the loose amount increased first. Then, it decreases with the increase of the angle between the maize and the airflow tube because the airflow force is easily lost on the surface, and the gap between the kernels and the loosening effect worsens. When the angle between the airflow and the maize increases, the air force on the kernel surface increases, and when the force reaches the critical value of the force chain, the maize kernel will be loosened.

As shown in Figure 6b, when the diameter of the air pipe was 8 mm, and the angle between the maize and the air pipe was constant, the loose amount rises first and then decreases with the increase of the air pipe flow rate. The reason was that the increase in the flow rate caused the airflow to exert uniform force on the surface of the kernel and enhance the impact force, which was conducive to the seed loosening. However, the applied force on the surface of the maize was not uniform, air was easily lost with the grain gap, and the loss effect could be better. The airflow rate was constant, and the loose amount rose first and then decreased with the increase in the angle between the maize and the airflow tube. The reason was that the angle between the maize and the airflow tube increased to a certain extent, and the airflow lost less in the gap, so the loose amount was reasonable. When the angle continued to increase, the impact force mainly acted on the maize cob, and the loose amount was poor.

As shown in Figure 6c, when the angle between the maize and the airflow tube was 45°, and the diameter of the airflow tube was constant, the loose amount increased first and then decreased with the airflow tube flow rate increase. The reason was that the impact force of increasing the flow rate dramatically impacts the force chain network, resulting in loose seeds. As the flow rate continued to increase, the surface flow rate of seeds became too fast. Part of the airflow was not fully acting on the kernel's surface and was lost in the gap, which does not affect the stability of the force chain network, and the loose amount is poor. When the air pipe's flow rate was constant, the number of loose kernels first decreased. Then, it rose with the increase in the air pipe's diameter because the cross-sectional area and flow increased with the growth of the air pipe's diameter, and the impact force weakened. This had little influence on the stability of the force chain network and poor loosening effect.

For maize threshing amount y, the interaction term between the air pipe's flow rate and the air pipe's diameter affected the maize's threshing amount, as shown in Figure 6d. When the angle between the ear of maize and the air pipe was 45°, and the diameter of the air pipe was constant, the threshing amount showed an upward trend with the increase of the flow rate of the air pipe. The reason was that the greater the flow rate, the stronger the impact force, and the force chain was easily broken. Threshing was realized when the impact force reached the critical value of breaking the kernel force chain network. When the flow rate was 31-33 m/s, the threshing quantity increased first and then decreased with the increase of the diameter of the air duct. When the diameter of the air duct was 6-8 mm, the threshing quantity of maize was significantly affected because the small diameter of the air duct, and the increase of the flow rate, significantly impacted the stability of the force chain network and was accessible to threshing. When the flow rate of the air duct was 34-35 m/s, and the diameter of the air duct was 9-10 mm, the threshing quantity was manageable. The reason was that the impact area increased with the increase of air pipe diameter and airflow rate, which affected the loose grain amount. However, it was not enough to damage the balance of the chain network, resulting in poor threshing amount.

According to Figure 7, the damage rate of the observed indicators was below 3%. The reason was that airflow threshing had an impact and pull effect on the kernel; the threshing effect was obvious, and the damage to the kernel was small.

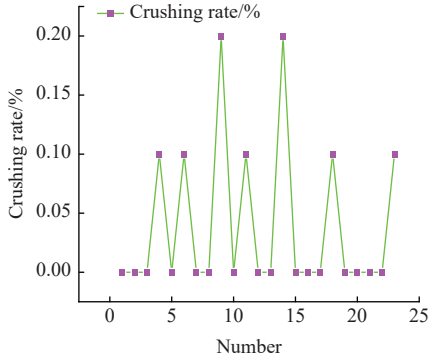

Figure 7 Line chart of observation indicators

4.4 Parameter optimization and test verification

Based on multi-factor experiments, the multi-objective optimization algorithm of Design-Expert 13.0 software was used to optimize the parameters, and the maximum loose amount and maximum threshing amount were taken as the objectives. The objectives and constraints were as follows:

$$\begin{cases} \max y_1 \\ \max y_2 \\ \text{s.t.} \begin{cases} 15^\circ \le x_1 \le 75^\circ \\ 6\ \text{mm} \le x_2 \le 10\ \text{mm} \\ 27\ \text{m/s} \le x_3 \le 35\ \text{m/s} \end{cases} \end{cases} \quad (8)$$

Two regression equation models were used for multi-objective optimization, and the optimal parameter combination was x_1=45°, x_2=7 mm, and x_3=33 m/s. Combined with the measurement of multi-dimensional force values above, it could be seen that the optimal parameters were as follows: transverse maize, the angle between the maize and the air compressor air pipe was 45°, the diameter of air compressor air pipe was 7 mm, the flow rate of air compressor air pipe was 33 m/s, the loose amount was 10 pieces, and the threshing amount was 15 pieces. These parameters resulted in the best threshing performance.

4.4.1 Forward analysis of the maize threshing process

The "arrangement law" composed according to the "staggered and lapping principle" is shown in Figure 8. The threshing area on the surface of the maize kernels is marked with different colors, as shown in Figure 8. The reference maize kernel 0 was taken as the research object, and the coordinate information of the kernel was tracked and saved. The selection interval of each picture was 2499.96 μs. A total of eight pictures were selected to show the threshing process of maize kernels under high-speed photography, as shown in Figure 8.

Based on the coordinate information of the threshing process as shown in Figure 9, MATLAB software was used to fit the motion process, and the fitting curve, shown in Figure 10, was obtained. The motion path type of maize kernels was found to be an inclined tossing motion. Under the action of airflow impact force and lift force, the maize kernels were driven to show a discrete and upward movement, as shown in Figures 9a-9e. Under the action of auxiliary airflow, the discrete maize kernels could be pushed and separated.

The maize kernels moved upward, coupled with air resistance, gravity, and other factors, as shown in Figures 9f-9h. In the initial dispersion of maize kernels, the velocity was maximum under the action of airflow impact force and lift force. In the threshing process, the velocity gradually decreased under the influence of the kernel's gravity and air resistance. When the position reached the highest point, there was only horizontal component velocity, which accelerates under gravity. Finally, the maize kernel velocity showed a rapid downward trend with the change of position, as shown in Figure 10. In the initial dispersion process, the direction of the maize kernel's gravity and air resistance was downward, so the direction of velocity and acceleration was opposite. With the increase of maize kernel acceleration, the direction of acceleration and velocity was gradually consistent. However, air resistance still affected it during movement, and the acceleration gradually decreased, as shown in Figure 10.

a. Threshing area color marking b. Threshing effect c. Arrangement units

Figure 8 Color marking and effect diagram of maize threshing area

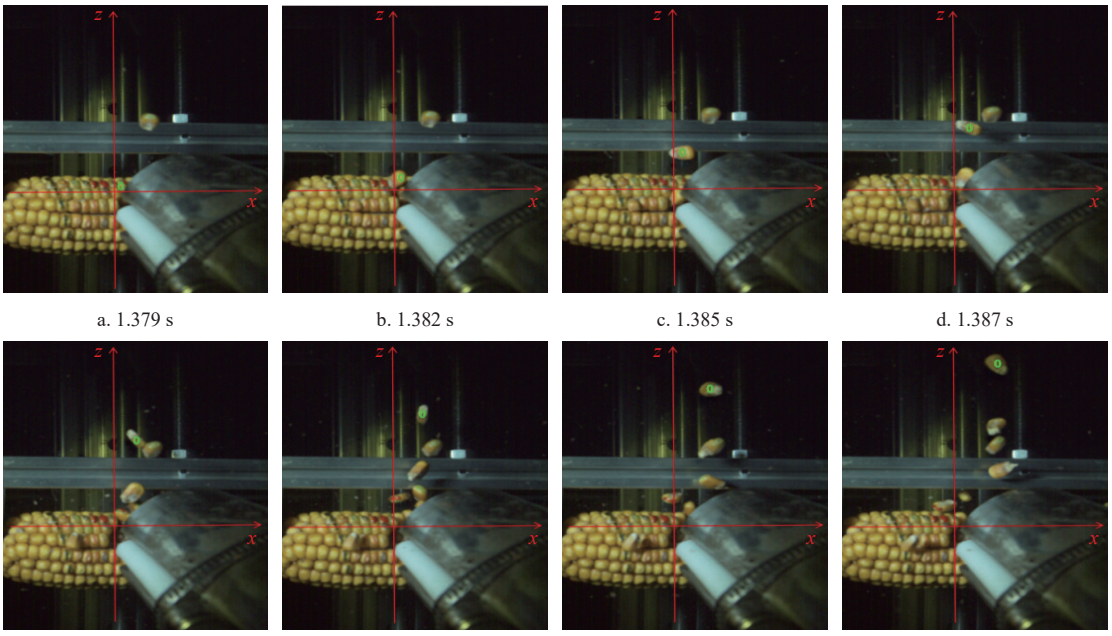

a. 1.379 s b. 1.382 s c. 1.385 s d. 1.387 s

e. 1.390 s f. 1.392 s g. 1.395 s h. 1.397 s

Figure 9 Analysis of maize grain motion under forward high-speed photography

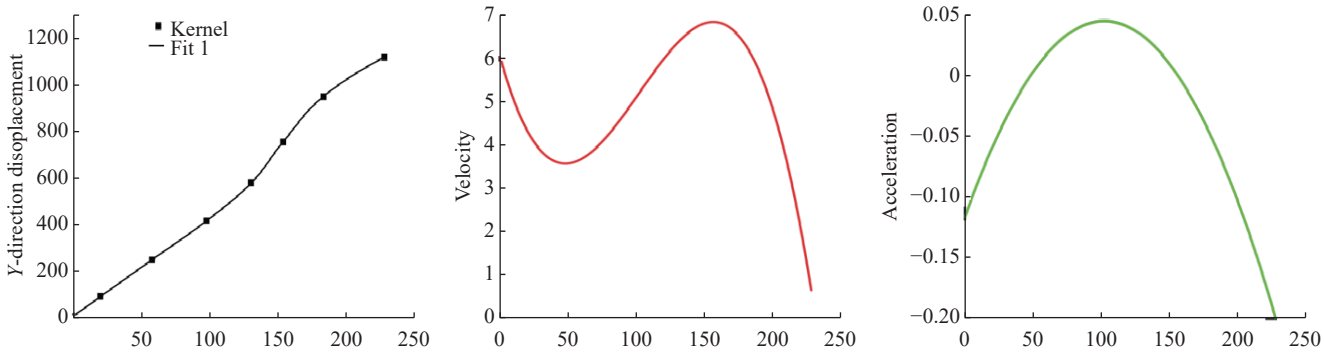

a.Displacement of maize kernel motion b.Speed of maize kernel movement c.Acceleration of maize kernel movement

Figure 10 Curve fitting of grain threshing movement

In Figure 9 and Figure 10, it was found that under the impact of airflow and lift force of reference maize kernel 0, the maize kernel had an upward pulling force, the balance of transverse and longitudinal force chains was destroyed, and the maize kernel began to disperse. After the maize kernels were threshed, airflow continuously impacted the surrounding maize kernels, resulting in

looser and threshed phenomena. Figure 9b and Figures 9e-9h found that other maize kernels were first threshed from a single maize kernel, and then the surrounding misplaced maize kernels were threshed along an axial spiral.

4.4.2 Analysis of maize threshing rule under lateral high-speed photography

To investigate the transfer of the force chain network and the maize kernel threshing rule under the optimized parameters of maize threshing and the impact of air coupling, the high-speed photography test was carried out from the side at 45°. High-speed photography extracted a photo every 0.02 s and selected eight images of maize kernels in threshing and loose states, as shown in Figure 11.

It could be seen from Figure 11 that under the coupled impact of airflow, the single kernel was first loosened and threshed, as shown in Figures 11a-11c, and the single maize kernel force chain network was broken. This was because the force would be transferred according to the closure of the transverse force chain network, forming a cyclic force circle. After the maize kernel falls off, the force chain would be broken, the cyclic force circle would be destroyed, the comprehensive force around it would weaken the maize kernel, and the maize kernel would gradually disperse.

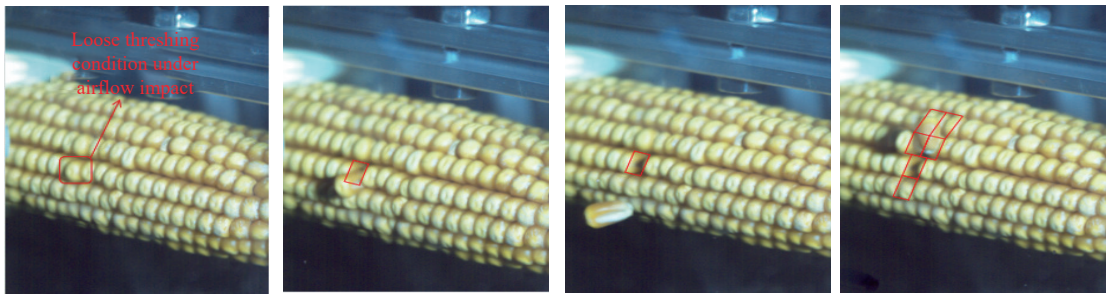

a. 8.250 s b. 8.275 s c. 8.300 s d. 8.350 s

e. 9.225 s f. 9.275 s g. 13.250 s h. 13.275 s

Figure 11 Rule of maize threshing under lateral high-speed photography

As shown in Figures 11d-11f, the maize force chain breaks due to the fact that the force will continue to be dispersed in the unit of arrangement units. It could be seen from Figures 11g-11h that under the continuous impact of airflow, the maize kernel was gradually threshed along the spiral closure direction of the surface of the maize in the unit of the arrangement, and so on, to finally achieve the threshing process. The force chain was based on the arrangement unit, and the force transfer process in the force chain is shown in Figure 12. The arrangement units were misaligned and overlapped. When an external force acts on them, the force is transmitted to each other along the arrangement units. During the transmission process, the force was affected by the superposition of maize kernels, and the force was gradually consumed.

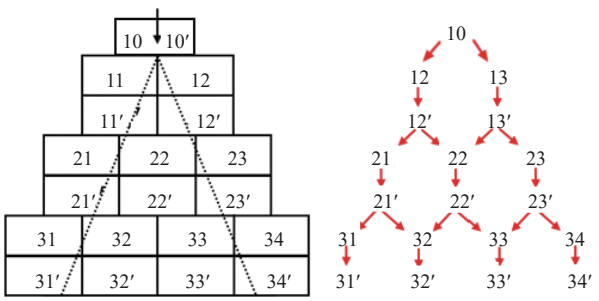

Figure 12 Composition of force chain and transfer process of force in force chain

5 Conclusions

1) It can be seen from the velocity changes of the flow field in the maize kernel thresh region that when the air strikes the maize surface, an accelerating air will form on its circular surface with an apparent velocity gradient. The airflow velocity was symmetrically distributed on the maize surface, indicating that the airflow velocity was stable. The velocity gradient and pressure gradient difference of the two types of airflow enable the low-speed airflow to wrap the high-speed airflow better and reduce airflow dissipation.

2) Through the visual smoke test of the airflow coupling state, it was found that the high-speed airflow can disrupt the low-speed airflow from the initial boundary disturbance to the gradual entrainment and then be wrapped entirely by the low-speed airflow. It was found that high-speed airflow has a strong breakdown ability. In contrast, the low-speed airflow as an auxiliary airflow could reduce the dissipation of the high-speed boundary airflow and improve the impact force. The low-speed airflow can play an auxiliary role, and the impact area was prominent. According to conclusion 1, the velocity variation of the simulated flow field and the airflow variation are consistent.

3) In the single-factor and multi-factor tests, it was found that the significant and minor order of influence of each factor on the loose amount of maize ear was x_3, x_2, and x_1, and the significant and minor order of influence on the loose amount of maize was x_3, x_2, and x_1, and the regression equation of each factor on the loose

amount and threshed amount was determined. Through parameter optimization, it was found that the optimal parameter combination was transverse maize, the angle between maize and air pipe was 45°, the diameter of the air compressor air pipe was 7 mm, the flow rate of the air compressor air pipe was 33 m/s, the loose amount was 10 pieces, the threshing amount was 15 pieces, and the damage rate was below 3%, which meets the actual threshing demand.

4) The forward and lateral high-speed photographic tests found that the transverse threshing movement was inclined, and the threshing trajectory and transfer process followed the "arrangement law". It was found that the cyclic force circle was destroyed after the maize kernel fell off. The maize kernel was threshed in the arrangement unit, and the threshing process was "spiral".

Acknowledgements

This work was funded by the National Natural Science Foundation of China (Grant No. 52275245) and the Henan Science and Technology Research Project (Grant No. 222103810041). This study could only be done with the help of the postgraduate students in the research team. The authors are grateful for the support of the fund project and the research team members.

[References]

[1] Zhu X L, Chi R J, Ma Y Q. Effects of corn varieties and moisture content on mechanical properties of corn. Agronomy, 2023; 13(2): 545.

[2] Xie R Z, Ming B, Gao S, Wang K R, Hou P, Li S K. Current state and suggestions for mechanical harvesting of corn in China. Journal of Integrative Agriculture, 2022; 21(3): 892–897.

[3] Li X P, Zhang W T, Xu S D, Du Z, Ma Y D, Ma F L, et al. Low-damage maize threshing technology and corn threshing devices: a review of recent developments. Agriculture, 2023; 13(5): 1006.

[4] Xu J, Meng J H, Quackenbush L J. Use of remote sensing to predict the optimal harvest date of corn. Field Crops Research, 2019; 236: 1–13.

[5] Ma Z, Han M, Li M Y, Yu C S, Chandio F A. Comparing kernel damage of different threshing components using high-speed cameras. Int J Agric & Biol Eng, 2020; 13(6): 215–219.

[6] Wang Y Z, Li L L, Gao S, Guo Y N, Zhang G Q, Ming B, et al. Evaluation of grain breakage sensitivity of maize varieties mechanically-harvested by combine harvester. Int J Agric & Biol Eng, 2020; 13(5): 8–16.

[7] Basuki M, Aprilyanti S, Azhari, Madagaskar. Design of corn thresher. In: 3RD forum in research, science, and technology(First 2019) international conference, Indonesia: 2020; 1500(1): 012075. doi: 10.1088/1742-6596/1500/1/012075.

[8] Yang L, Cui T, Qu Z, Li K. H, Yin X W, Han D D, et al. Development and application of mechanized maize harvesters. Int J Agric & Biol Eng, 2016; 9(3): 15–28.

[9] Fu J, Chen Z, Han L J, Ren L J. Review of grain threshing theory and technology. Int J Agric & Biol Eng, 2018; 11(3): 12–20.

[10] Zhang N, Fu J, Wang R X, Chen Z, Fu Q K, Chen X G. Experimental study on the particle size and weight distribution of the threshed mixture in corn combine harvester. Agriculture, 2022; 12(8): 1214.

[11] Yang L Q, Lü Q Q, Zhang H M. Experimental study on direct harvesting of corn kernels. Agriculture, 2022; 12(7): 919.

[12] Steponavicius D, Puzauskas E, Spokas L, Jotautiene E, Kemzuraite A, Petkevicius S. Concave design for high-moisture corn ear threshing. Mechanika, 2018; 24(1): 80–91.

[13] Dong J Q, Cui T, Zhang D X, Yang L, He X T, Jing M S, et al. Development of a low-damage maize threshing system based on discrete element technology to effectively improve maize harvest quality and yield. Powder Technology, 2024; 448: 120297.

[14] Mousaviraad M, Tekeste M Z. Systematic calibration and validation approach for discrete element method (DEM) modeling of corn under varying moisture contents (MC). Journal of the ASABE, 2024; 67(2): 259–274.

[15] Feng X, Wang L J, Bi S Y, Wang B, Ma Z, Gao Y P. Effects of threshing devices, maize varieties and moisture content of grains on the percentage of maize grains broken in harvesting. Agronomy, 2023; 13(6): 1615.

[16] Ghafori H, Hemmat A, Borghaee A M, Minaei S. Physical properties and conveying characteristics of corn and barley seeds using a suction-type pneumatic conveying system. African Journal of Agricultural Research, 2011; 6(27): 5972–5977.

[17] Nguyen T T, Rosselló C, Ratti C. Simple mathematical modelling to represent air-drying kinetics of potato peel. Journal of Food Engineering, 2023; 357: 6.

[18] Chai X Y, Zhou Y, Xu L Z, Li Y, Li Y M, Lv L Y. Effect of guide strips on the distribution of threshed outputs and cleaning losses for a tangential-longitudinal flow rice combine harvester. Biosystems Engineering, 2020; 198: 223–234.

[19] Shang Y, Wang C, Xu H, Liu S, Jiang W, Dong J. Noise source identification of the grain combining harvester based on acoustic array test. Applied Engineering in Agriculture, 2020; 36(6): 879–890.

[20] Zhao J L, Zhao H, Tang H, Wang X G, Yu Y J. Bionic threshing component optimized based on MBD-DEM coupling simulation significantly improves corn kernel harvesting rate. Computers and Electronics in Agricultural, 2023; 212: 108075.

[21] Zhang H, Chen B, Li Z J, Zhu C H, Jin E, Qu Z. Design and simulation analysis of a reverse flexible harvesting device for fresh corn. Agriculture, 2022; 12(11): 1953.

[22] Yang F, Du Y F, Fu Q F, Li X Y, Li Z, Mao E R, et al. Design and testing of seed maize ear peeling roller based on Hertz theory. Biosystems Engineering, 2021; 202: 165–178.

[23] Dong J Q, Zhang D X, Yang L, Cui T, Zhang K L, He X T, et al. Discrete element method optimisation of threshing components to reduce maize kernel damage at high moisture content. Biosystems Engineering, 2023; 233: 221–240.

[24] Li X P, Du Z, Ma Y D, Gao L X. Bare hand threshing experiment on corn ear kernel. Asian Association for Agricultural Engineering, 2014; 23(3): 74–80.

[25] Li X P, Xiong S, Ma L, Jin X, Ji J T. High-speed camera analysis of seed maize ear bare hand threshing. Asian Association for Agricultural Engineering, 2017; 26(1): 60–67.

[26] Li M T, Wen X Y, Zhou F J. Working parameters optimization and experiment of precision hole fertilization control mechanism for intertilled crop. Transactions of the CSAM, 2016; 47(9): 37–43. (in Chinese)

[27] Zhu X L, Chi R J, Du Y F, Qin J H, Xiong Z X, Zhang W T, et al. Experimental study on the key factors of low-loss threshing of high-moisture maize. Int J Agric & Biol Eng, 2020; 13(5): 23–31.